J. Chem. Sci. (2019) 131:33
https://doi.org/10.1007/s12039-019-1608-7

REGULAR ARTICLE

Influence of TiO_2 structural properties on photocatalytic hydrogen gas production

HASLIZA BAHRUJI[a,*], MICHAEL BOWKER[b,c] and PHILIP R DAVIES[b]

[a]Centre of Advanced Material and Energy Science, University Brunei Darussalam, Jalan Tungku Link, Gadong BE 1410, Brunei Darussalam
[b]School of Chemistry, Cardiff Catalysis Institute, Cardiff University, Main Building, Cardiff CF10 3AT, UK
[c]UK Catalysis Hub, Research Complex at Harwell (RCaH), Rutherford Appleton Laboratory, Harwell, Oxon OX11 0FA, UK
E-mail: hasliza.bahruji@ubd.edu.bn

MS received 18 December 2018; revised 12 February 2019; accepted 14 February 2019; published online 26 March 2019

Abstract. A range of commercially produced TiO_2 was deposited with Pd nanoparticles and the activities of the anaerobic, ambient temperature photocatalytic hydrogen production from water-methanol mixture were evaluated. The photocatalytic reactions were carried out in the liquid and gas phase conditions with the rate of hydrogen evolutions were higher was when in the gas phase. The Pd/TiO_2 catalysts were characterised using XRD, N_2 adsorption, infrared and XPS in order to investigate the influence of structural properties of TiO_2 in determining photocatalytic activity. A positive relationship was established in the rate of hydrogen production from the gas and liquid phase conditions with the size of crystallite TiO_2. Analysis of the surface properties of TiO_2 using XPS shows the presence of surface hydroxyl that also influenced the photocatalytic activity of TiO_2.

Keywords. Photocatalysis; hydrogen production; methanol; alcohol reforming; titania-Pd catalysts.

1. Introduction

Hydrogen gas can be a useful energy carrier, and an economy based on hydrogen as a fuel is a real possibility for the future. Current production of hydrogen is mostly from fossil fuels and fuel processing of methane is the most common hydrogen production method in industries.[1] Generation of hydrogen from clean and sustainable resources namely, water has received a great deal of attention particularly to increase the efficiency of the process and the viability for commercialization. One of industrial application is using high-temperature electrolysis for hydrogen that shows the advantage of isolating hydrogen gas from water.[2] Photocatalytic water splitting also offers a sustainable route to produce H_2 from water and such a possibility was presaged by the work of Fujishima and Honda.[3] The most promising semiconductor that offers stability, high activity and non-toxicity is TiO_2 but the activity is restricted by the 3.2 eV band gap equivalent to a maximum wavelength of $\sim$ 388 nm which means that only $\sim$ 5% of the light arriving on the surface of the Earth is capable of initiating the reaction. A significant increase in research on developing novel semiconductors for photocatalytic water splitting has occurred in recent times with the aim of narrowing the band gap and utilizing a wider range of photon energy within the solar spectrum.[4–7] Doped-TiO_2 with either metal or non-metal dopant showed improved activities than TiO_2 with some of the new materials shifting band gaps and increasing absorption into the visible light region.[8–10] Engineering of TiO_2 structures to form Ti^{3+} core/Ti^{4+} shell enhanced the photocatalytic activity of rutile TiO_2 for hydrogen production.[11] The formation of nanostructured TiO_2 hollow sphere inhibits the recombination of the energy carriers and increases the adsorption of the organic substrate for the high photocatalytic performance of TiO_2.[12] The interfacial charge transfer between TiO_2 and co-catalyst is important which can be influenced by the crystal face of TiO_2 and the degree of crystallinity of the interlayer.[13] Another concern that needs to be addressed is the facile nature of the back reaction between oxygen and hydrogen. Organic sacrificial agents can be added to capture the highly active oxygen species produced, thus avoiding such recombination.[14] In a previous work, we have studied the hydrogen gas production from palladium

*For correspondence

nanoparticles impregnated onto TiO_2 and gained important insights into the role of the Pd nanoparticles in the system. Apart from improving the electron-hole separation, Pd also provides active sites for reaction.[15,16] P25 TiO_2 from Evonik is a standard semiconductor used for this reaction, and it has been proposed that the activity fundamentally relies on the synergistic effects occurring between anatase and rutile phases.[17,18] In the photocatalytic reaction, the charge migration to the surface is crucially important to avoid bulk recombination and can be improved by reducing the diameter of the particles; in other words, the length of the electron needs to travel to reach the surface. Once on the surface, the charges can be trapped, involved in the photoreaction or recombined. For most of the metal oxides such as TiO_2, the surface is covered with hydroxyl groups and it is believed these groups can play a role in enhancing surface reaction by trapping the photogenerated holes, producing $OH^{\bullet}$ radicals.[19]

In this study, we have investigated a range of TiO_2 powders obtained commercially with a variation of surface area and crystallite size in order to further understand the properties that determine the activity of TiO_2 to generate hydrogen from the photocatalytic reformation of methanol. After the deposition with palladium nanoparticles and calcination at 500 °C, the catalysts were characterized using XRD, infrared, N_2 adsorption and XPS analysis. The influence of reaction conditions were also studied by carrying out the experiments in the liquid and gas phase conditions.

2. Experimental

2.1 *Materials and method*

The TiO_2 powders obtained from commercial provider used were as follows; **P25** was obtained from Evonik, which was prepared *via* the flame synthesis method using $TiCl_4$ as the Ti source. **HombifineN** was obtained from Sachtleben Chemie GmbH, Germany. TiO_2 **PC500** was obtained from Millenium Inorganic Chemical **S.A.**, an ultrafine powder with high surface area and low sulphate content. **NanoTiO$_2$** was obtained from UCL which was produced in a continuous hydrothermal flow synthesis (CHFS) reactor.[20,21] The synthesis was carried out was using Titanium (IV) bis(ammonium lactato)dihydroxide as Ti precursor. Altair TiO_2 powder was purchased from **Altair**, which was produced by spray hydrolysis of concentrated Ti followed by an annealing and milling processes. The Ti was extracted from ilmenite ore in concentrated hydrochloric acid.[22] This type of TiO_2 is often used as a pigment in paint. Pd was deposited on each titania *via* an incipient wetness impregnation. 0.01 g of $PdCl_2$ was dissolved in acidified water and the solution was added gradually to 2 g titania and subsequently dried at 200 °C for 2 h and then at 500 °C for 3 h. Samples were ground and sieved to an aggregate size of less than 53 μm.

2.2 *Photocatalytic reaction*

Photocatalytic methanol reforming experiments were carried out in both the liquid and the gas phase conditions under the UV region (240–380 nm). In the liquid phase experiment, the catalyst (0.2 g), methanol (100 μL, Aldrich 99.9%) and water (deionised, 100 mL) were added directly to the reaction vessel and stirred during the reaction. For the gas phase experiments, the same mass of a catalyst (0.2 g) was pressed onto an area of approximately 4 cm^2 of a glass slide. The slide was placed with the bottom of the catalyst area approximately 2 cm above the water/methanol mixture. In both types of the experiment the methanol/water mixture was purged with Ar for 30 min to remove air and the flask illuminated by a 400 W Xe arc lamp (Oriel model 66921). Gas samples were taken every 30 min and analysed by Varian 3900 GC using a 2 m MS 13X column. Control experiments were carried out with all identical conditions, but in the absence of the catalyst. This yielded no significant hydrogen evolution.

2.3 *Characterisation of the catalysts*

XRD patterns were obtained using an Enraf Nonus FR590 diffractometer fitted with a hemispherical analyzer, using Cu K α radiation ($\lambda = 1.54$ Å). XPS spectra were obtained using a Kratos Axis Ultra-DLD spectrometer system utilising a monochromatic Al k α source and at 40 and 160 eV for high resolution and survey scans respectively. XPS data was analyzed using CasaXPS v2.3.16 using sensitivity factors supplied by the manufacturer.[23] The signal has been resolved by a curve fitting procedure using Gaussian/ Lorentzian fits. BET surface areas were obtained using a Micromeritics Gemini 2360 in a static volumetric method.

3. Results and Discussion

XRD analysis shown in Figure 1 indicated the presence of peaks at 25.3°, 36.1°, 37.8°, 39.2°, 41.2°, 44.0°, 48.1°, 54.2°, 62.5°, 69.0°, 70.0° and 75.1° associated with the anatase crystal plane (JCPDS card No 21-1272). These peaks were observed on all TiO_2 powders, NanoTiO_2, PC 500, Hombifine N, Altair and P25. TiO_2 P25, however, showed peaks associated with rutile crystal plane at 27.4°, 38.6° and 47.9° indicating the presence of anatase and rutile mixture in P25 (JCPDS card no. 21-1276). From the FHWM of 25.3° [101] peaks, the average particle sizes were calculated using the Debye-Scherrer equation and the values are given in Table 1. NanoTiO_2 appeared as TiO_2 with the smallest crystallite with an estimated size of 8 nm meanwhile Altair TiO_2 crystallite

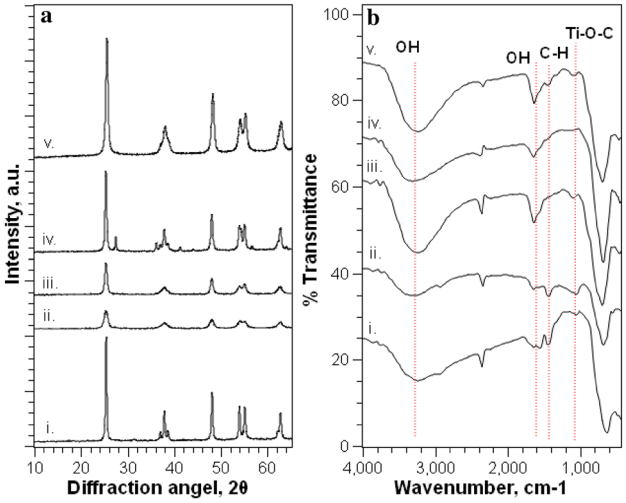

Figure 1. (a) X-ray diffraction pattern; and (b) ATR-FTIR spectra of TiO_2 with 0.3% Pd wt. loading following calcination in air at 500 °C; i. Altair; ii. Nano TiO_2; iii. HombifineN, iv. P25 and v. PC500.

size is the largest with an estimated value of 27 nm. The surface area of the TiO_2 following deposition with Pd was also measured using N_2 adsorption analysis. The BET surface area analysis of the samples summarized in Table 1 shows that the catalysts have a range of surface area from 47 $m^2\ g^{-1}$ for Altair to 101 $m^2\ g^{-1}$ for NanoTiO_2.

The ATR-infrared analysis of TiO_2 was illustrated in Figure 1b revealed the presence of a functional group that may affect the catalytic performance. The characteristic peaks of absorbing hydroxyl stretching vibrations appear at 3200 cm^{-1} and 1644 cm^{-1}. The hydroxyl adsorption bands indicate the presence of surface hydroxyl as well as adsorbed water molecule on the TiO_2 surface. It is, however, difficult to distinguish between surface hydroxyl and adsorbed water molecules due to the infrared analysis that was carried out in an open environment. The small peak that appeared at 1424 cm^{-1} corresponded to the vibrations of Ti-O-C that may have originated from titanium precursor that contained carbon during the synthesis or surface carbonate species that were formed by adsorbed atmospheric CO_2 on the TiO_2 surface.[24] A broad peak centred at 640 cm^{-1} is originating from Ti-O-Ti vibration attributed to the presence of TiO_2 framework.[25]

The TiO_2 was also analyzed using XPS to investigate the surface properties that may influence the discrepancy of TiO_2 photoactivity in hydrogen generation. The XPS spectra of the TiO_2 following deposition with Pd and calcination in air at 500 °C in Figure 2a and 2b showed peaks in the Ti $2p_{3/2}$ and O 1s regions at 459 eV and 529.6 eV respectively, indicative of titania with Ti in the 4+ oxidation state[26] with Ti:O ratios in the range of 1:1.6 to 1:1.8 for all powders. The asymmetric O1s peak observed on all samples imply the presence of more than one state of oxygen and the spectra have been resolved into three oxygen components. The most intense peak appears at 529.6 eV, corresponding to oxygen in the metal oxide,[27] while the peak at 531.0 eV is characteristic of surface hydroxyl groups, OH.[28,29] A relatively small peak at 532.8 can be attributed to adsorbed molecular water. From the XPS analysis, we can determine the density of surface hydroxyl groups on the TiO_2 relative to the total lattice oxygen, OH/O^{2-} [30,31] and these data are given in Table 1. Pd 3d signal was also observed on the catalysts as shown in Figure 2c. The peak appeared at 336.0 eV corresponded to PdO signal. There are no significant differences in Pd binding energy between the Pd/TiO_2 catalysts.

The TiO_2 deposited with 0.3% wt Pd was evaluated for photocatalytic hydrogen production in the liquid phase and gas phase reactions. The amount of hydrogen produced from methanol-water mixtures within three hours of reactions were shown in Figure 3. All catalysts were active without apparent induction period for H_2 production. Photocatalytic reaction in liquid phase condition showed that Pd deposited on nanoTiO_2 produced a low volume of hydrogen with only ~ 48 μmol of H_2

Table 1. Structural properties of Pd/TiO_2 catalysts measured by XRD, N_2 adsorption and XPS analysis.

	P25	NanoTiO_2	PC 500	HombifineN	Altair
Crystalline phase	Rutile Anatase	Anatase	Anatase	Anatase	Anatase
Size, nm	22	8	16	14	27
Surface area, m^2/g	52	97	86	101	46
Rate of H_2, $\mu mol.s^{-1}.m^{-2}$					
Liquid	9.21	0.15	2.70	2.08	6.64
Gas	12.05	2.52	6.28	3.27	14.05
*Surface hydroxyl, OH/O^{2-}	0.14	0.24	0.16	0.23	0.19

*Calculated from O1s XPS data.

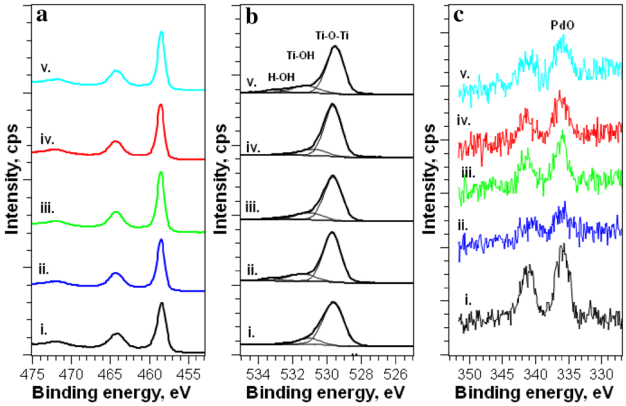

Figure 2. XPS analysis of TiO_2 with 0.3% wt. Pd following calcination at 500 °C for 3 h; (a) Ti2p XPS region, (b) Oxygen 1s photoelectron spectra with a curve fitted analysis of its components at 529.6 eV for lattice oxygen, Ti-O; 531.5 eV assigned for a surface hydroxyl group, Ti-OH; 533 eV for an adsorbed water molecule, (c) Pd 3d XPS spectra of the catalysts. (i. 0.3% Pd on P25 TiO_2; ii. 3% Pd on PC500 TiO_2; iii. 3% Pd on P25 TiO_2; iv. 3% Pd on HombifineN TiO_2; v. 3% Pd on Nano TiO_2).

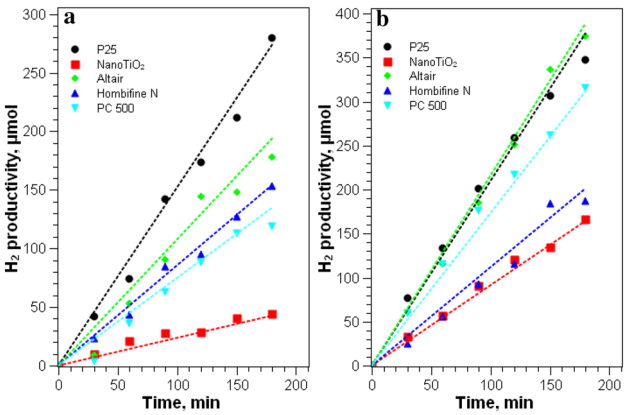

Figure 3. Plot of H_2 gas production from Pd/TiO_2 catalysts under UV region in (a) Liquid phase reaction condition; (b) Gas phase reaction condition.

was produced in 3 h under UV light irradiation. The hydrogen gas production was gradually increased from nanoTiO_2 < Hombifine N < PC 500 < Altair < P25; with P25 appeared as the most active catalyst to give ~ 279 µmol of H_2 in 3 h. The photocatalytic reaction was further attempted in the gas phase condition, where the catalysts were mounted on the glass slide and positioned above the methanol-water mixture to allow interaction of the catalysts with water and methanol vapors. Figure 3b showed the plot of hydrogen gas production over irradiation time. The hydrogen volume from all the Pd/TiO_2 catalysts were higher than the reaction carried out in the liquid phase. Altair and P25 TiO_2 showed similar activity towards hydrogen production contrary to the reaction in the liquid phase. Pd supported on PC500 TiO_2 also showed enhanced activity with ~ 315 µmol of H_2 produced within 3 h of reaction. As observed in the liquid phase condition, the highest surface area catalyst, NanoTiO_2 is the least active catalysts with ~ 166 µmol of hydrogen produced in 3 h. The rate of hydrogen evolution for all catalysts were calculated and summarized in Table 1.

Photocatalytic hydrogen gas production from the methanol-water mixture is an ideal way to produce hydrogen from sustainable resources using energy from sunlight. The reaction involves a stoichiometric reaction between one mole of methanol with one mole of water to form 3 mole of H_2 gases and CO_2.[32]

$$CH_3OH(l) + H_2O \rightarrow CO_2(g) + 3H_2\,(g) \quad (1)$$

In this study, we showed that the rate of hydrogen generation occurs at a significantly faster rate in the gas phase condition, in comparison to the reaction in the liquid phase condition. All the catalysts were more active in the gas phase and almost double the amount of hydrogen was produced in three hours, the exception being P25 which showed only a 25% increase in rate. The most likely explanation for this is that the vapor pressure of methanol is relatively higher than water.[33] This subsequently reduced water concentration in the gas phase and enhanced methanol concentration and adsorption on the surface of the catalyst. The presence of methanol is crucial for initiating hydrogen gas evolution with methanol adsorption/reaction on Pd/TiO_2 can be a rate-limiting step for the overall reaction. Methanol acts as a hole scavenger to allow the electron to be used for the generation of oxygen vacancies for water reduction. Studies of water and methanol adsorption on the TiO_2 surfaces by Wang *et al.,* showed that CH_3OH is strongly adsorbed on the TiO_2 surface in the gas phase conditions.[34] Shen *et al.,* have demonstrated that methanol decomposition occurs *via* proton transfer from methanol to the oxygen bridging, O_{br} on TiO_2 surfaces.[35] The presence of excess water molecules occupying the O_{br} sites inhibited proton transfer and hence may explain the slower hydrogen production rates in the liquid phase condition. We also suggested that in the gas phase condition, Pd/TiO_2 catalysts have a direct exposure towards light irradiation without attenuation that arises from catalysts suspension as in liquid phase condition.[10] This may contribute to the efficiency of photon adsorption by catalysts that affect the catalytic performance.

Understanding the influence of TiO_2 on producing hydrogen from the water-methanol mixture, it is important to note that TiO_2 itself is almost inactive for catalyzing the reaction. Following the deposition of Pd nanoparticles, the catalyst was immediately active in the

liquid phase photo-reforming reaction. The high rates of hydrogen production over P25 have been attributed to the presence of the rutile component that provides a sink for photogenerated electrons, thus improving electron-hole separation.[17,18,36] The synergistic effect of rutile and anatase relies on the proximity between rutile and anatase components.[37] However, hydrogen was also produced at a relatively rapid rate from the catalysts that only consist of the anatase crystalline phase. Altair, PC500 and HombifineN produced ~ 150 µmol in three hours which is approximately half the amount produced from P25. NanoTiO_2 on the other hand, which possesses the second highest surface area of the samples, has a hydrogen production of only 43 µmol. The activities of P25 and Altair in the gas phase are very similar with around 350 µmol of hydrogen produced. Since Altair has no rutile component, the advantage of the presence of an anatase/rutile interface is called into question.

Table 1 shows the physical structure of the materials used in this study obtained from XRD, XPS and N_2 adsorption analysis. After making a detailed observation on the surface area of the catalysts, we observed that the rate of hydrogen production decreased on the catalysts with a larger surface area. In general, higher surface area catalysts would be associated with higher activity but in this case, the opposite trend is apparent. To gain further insight into the reasons for this behavior, we correlated the average crystallite size of the catalysts calculated from the XRD data with the specific activity of the catalysts (the rate of hydrogen evolution per unit area). The specific activity of the catalysts were determined by dividing the rate of hydrogen over the area of the catalysts, in order to obtain a fair comparison between the catalysts. Figure 4a shows the plot of the specific activity of the catalyst over crystallite size. Here the specific activity increased for larger particles; this effect is strong enough to dominate despite the increased total number of sites available on the smaller particles. Understanding the factors contributing to the observation, we relate the activity of the catalysts with the distance that the photogenerated electron and hole have to travel to reach the surface of the catalyst. Once initiated, the photogenerated electron-hole pair must be separated to prevent recombination. Studies on the dynamics of charge carrier trapping and recombination on colloidal TiO_2 with an average diameter of ~ 6 nm revealed that the trapping of electron occurs a lot faster than the trapping of hole.[38] The recombination of hole and electron however occurs at a much slower rate than the trapping.[38] Once the photogenerated hole was trapped, the charge carrier recombination process occurs at a much slower rate from picosecond to nanosecond.[39]

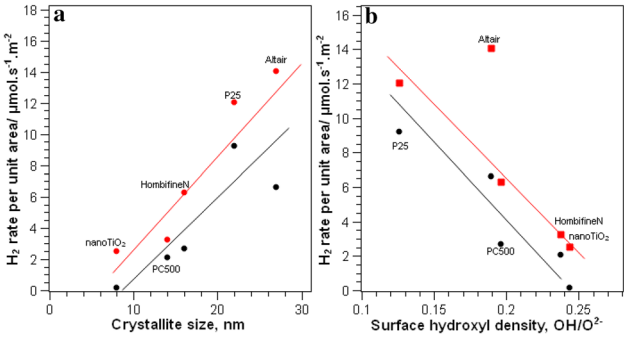

Figure 4. (a) Correlation between the rates of hydrogen production with the crystallite size of the catalysts; (b) The relationship between the rates of hydrogen production with the surface hydroxyl density (OH/O^{2-}) of TiO_2 with 0.3% Pd loading ● reaction in the gas phase; ■ reaction in the liquid phase.

With small particles, there is a confinement issue and the probability of e^- and h^+ recombination increased as particle size decreased.[40] Furthermore, for smaller particle sizes there is also more surface available, where the hole (h^+) can be trapped by reaction with OH^-(a) a process that typically occurs on a timescale of 100 ps to 10 ns.[41] The OH^- which traps the holes can come from surface bound water or the hydroxyl species present on the TiO_2 surface[42,43] and form trapped hole states and subsequently peroxo-titanium complexes.[44] Both the trapped hole states and the surface-bound peroxo-titanium were identified as recombination centers for charge carriers that decreased the efficiency of the photoreaction. To examine whether this factor also affects the present case, we have derived the surface hydroxyl over lattice oxygen ratios, OH/O^{2-} from the different catalysts using the curve fitting of the O1s XPS data. XPS is a surface sensitive catalysts and since catalytic reaction often occurs on the surface, this represents the active sites for trapping the photogenerated holes. We must bear in mind that the change in surface area/bulk ratio would necessarily also change the OH/O^{2-} ratio in XPS. Therefore, the relevant factor here is OH surface density which represents by the OH/O^{2-} ratios. It is apparent that the specific activity of the catalysts showed an indirect relationship with the surface hydroxyl/bulk oxygen ratio as shown in Figure 4b. The observation applies to both the gas and the liquid phase processes. This suggests that the relationship between the activities with the crystallite size in Figure 4 is a direct result of the smaller nanoparticle size that consists of high level of recombination centers and the electron-hole confinement issue that determines the changes in reactivity with size.

4. Conclusions

All of the catalysts investigated were more active in the gas phase and produced hydrogen in the presence of Pd nanoparticles. The activity of the catalysts is related to the size of the TiO_2 crystallite, despite being randomly obtained commercially. Although the catalysts with smaller particles may allow for more rapid migration of the charge carriers to the surface, the rate of charge recombination is also increased due to high level of recombination sites and electron-hole confinement issues.

References

1. Holladay J D, Hu J, King D L and Wang Y 2009 An overview of hydrogen production technologies *Catal. Today* **139** 244
2. Posdziech O, Schwarze K and Brabandt J 2018 Efficient hydrogen production for industry and electricity storage via high-temperature electrolysis *Int. J. Hydrogen Energy* https://doi.org/10.1016/j.ijhydene.2018.05.169
3. Fujishima A and Honda K 1972 Electrochemical photolysis of water at a semiconductor electrode *Nature* **238** 37
4. Subramanian E, Baeg J-O, Lee S M, Moon S-J and Kong K-j 2009 Nanospheres and nanorods structured Fe_2O_3 and $Fe_{2-x}Ga_xO_3$ photocatalysts for visible-light mediated ($\lambda >= 420$ nm) H_2S decomposition and H_2 generation *Int. J. Hydrogen Energy* **34** 8485
5. Kato H, Asakura K and Kudo A 2003 Highly efficient water splitting into H_2 and O_2 over lanthanum-doped $NaTaO_3$ photocatalysts with high crystallinity and surface nanostructure *J. Am. Chem. Soc.* **125** 3082
6. Bhatt M D and Lee J S 2017 Nanomaterials for photocatalytic hydrogen production: from theoretical perspectives *RSC Adv.* **7** 34875
7. She X, Wu J, Xu, H, Zhong J, Wang Y, Song Y, Nie K, Liu Y, Yang Y, Rodrigues M-T F, Vajtai R, Lou J, Du D, Li H and Ajayan P M 2017 High Efficiency Photocatalytic Water Splitting Using 2D $\alpha-Fe_2O_3/g-C_3N_4$ Z-Scheme Catalysts *Adv. Energy Mater.* **7** 1700025
8. Xie W, Li R and Xu Q 2018 Enhanced photocatalytic activity of Se-doped TiO_2 under visible light irradiation *Sci. Rep.* **8** 8752
9. Liu S-H, Tang W-T and Lin W-X 2017 Self-assembled ionic liquid synthesis of nitrogen-doped mesoporous TiO_2 for visible-light-responsive hydrogen production *Int. J. Hydrogen Energy* **42** 24006
10. Pelaez M, Nolan N T, Pillai S C, Seery M K, Falaras P, Kontos A G, Dunlop P S M, Hamilton J W J, Byrne J A, O'Shea K, Entezari M H and Dionysiou D D 2012 A review on the visible light active titanium dioxide photocatalysts for environmental applications *Appl. Catal. B Environ.* **125** 331
11. Yang Y, Liu G, Irvine J T S and Cheng H-M 2016 Enhanced photocatalytic H2 production in core–shell engineered rutile TiO_2 *Adv. Mater.* **28** 5850
12. Seadira T W P, Sadanandam G, Ntho T, Masuku C M and Scurrell M S 2018 Preparation and characterization of metals supported on nanostructured TiO2 hollow spheres for production of hydrogen via photocatalytic reforming of glycerol *Appl. Catal. B Environ.* **222** 133
13. Kemnade N, Gebhardt P, Haselmann G M, Cherevan A, Wilde G and Eder D 2018 How to evaluate and manipulate charge transfer and photocatalytic response at hybrid nanocarbon–metal oxide interfaces *Adv. Funct. Mater.* **28** 1704730
14. Higashimoto S, Hikita K, Azuma M, Yamamoto M, Takahashi M, Sakata Y, Matsuoka M and Kobayashi H 2017 Visible light-induced photocatalysis on carbon nitride deposited titanium dioxide: hydrogen production from sacrificial aqueous solutions *Chin. J. Chem.* **35** 165
15. Bahruji H, Bowker M, Davies P R, Kennedy J and Morgan D J 2015 The importance of metal reducibility for the photo-reforming of methanol on transition metal-TiO2 photocatalysts and the use of non-precious metals *Int. J. Hydrogen Energy* **40** 1465
16. Bahruji H, Bowker M, Davies P R and Pedrono F 2011 New insights into the mechanism of photocatalytic reforming on Pd/TiO_2 *Appl. Catal. B Environ.* **107** 205
17. Bickley R I, Gonzalez-Carreno T, Lees J S, Palmisano L and Tilley R J D 1991 A structural investigation of titanium dioxide photocatalysts *J. Solid State Chem.* **92** 178
18. Carneiro J T, Savenije T J, Moulijn J A and Mul G 2011 How phase composition influences optoelectronic and photocatalytic properties of TiO_2 *J. Phys. Chem. C* **115** 2211
19. Munuera G, Rives-Arnau V and Saucedo A 1979 Photo-adsorption and photo-desorption of oxygen on highly hydroxylated TiO_2 surfaces. Part 1.—Role of hydroxyl groups in photo-adsorption *J. Chem. Soc. Faraday Trans. 1 Phys. Chem. Condensed Phases* **75** 736
20. Chen M, Ma C Y, Mahmud T, Darr J A and Wang X Z 2011 Modelling and simulation of continuous hydrothermal flow synthesis process for nano-materials manufacture *J. Supercrit. Fluids* **59** 131
21. Gruar R I, Tighe C J and Darr J A 2013 Scaling-up a Confined jet reactor for the continuous hydrothermal manufacture of nanomaterials *Ind. Eng. Chem. Res.* **52** 5270
22. Dijkstra M F J, Panneman H J, Winkelman J G M, Kelly J J and Beenackers A A C M 2002 Modeling the photocatalytic degradation of formic acid in a reactor with immobilized catalyst *Chem. Eng. Sci.* **57** 4895
23. http://www.casaxps.com/.
24. Connor P A, Dobson K D and McQuillan A J 1999 Infrared spectroscopy of the TiO2/aqueous solution interface *Langmuir* **15** 2402
25. Yang, J, Bai H, Tan X and Lian J 2006 IR and XPS investigation of visible-light photocatalysis—nitrogen–carbon-doped TiO_2 film *Appl. Surf. Sci.* **253** 1988
26. Carley A F, Chalker P R, Riviere J C and Roberts M W 1987 The identification and characterisation of mixed oxidation states at oxidised titanium surfaces by analysis of X-ray photoelectron spectra *J. Chem. Soc. Faraday Trans. 1 Phys. Chem. Condensed Phases* **83** 370

27. Kumar P M, Badrinarayanan S and Sastry M 2000 Nanocrystalline TiO_2 studied by optical, FTIR and X-ray photoelectron spectroscopy: correlation to presence of surface states *Thin Solid Films* **358** 122
28. Yu J, Zhao X and Zhao Q 2000 Effect of surface structure on photocatalytic activity of TiO_2 thin films prepared by sol-gel method *Thin Solid Films* **379** 7
29. Regonini D, Jaroenworaluck A, Stevens R and Bowen C R 2010 Effect of heat treatment on the properties and structure of TiO_2 nanotubes: phase composition and chemical composition *Surface Interf. Anal.* **42** 139
30. Erdem B, Hunsicker R A, Simmons G W, Sudol E D, Dimonie V L and El-Aasser M S 2001 XPS and FTIR surface characterization of TiO_2 particles used in polymer encapsulation *Langmuir* **17** 2664
31. Jensen H, Soloviev A, Li Z and Søgaard E G 2005 XPS and FTIR investigation of the surface properties of different prepared titania nano-powders *Appl. Surface Sci.* **246** 239
32. Al-Mazroai L S, Bowker M, Davies P, Dickinson A, Greaves J, James D and Millard L 2007 The photocatalytic reforming of methanol *Catal. Today* **122** 46
33. Bahruji H, Bowker M, Davies P, Morgan D, Morton C A, Egerton T, Kennedy J and Jones W 2014 Rutile TiO_2–Pd photocatalysts for hydrogen gas production from methanol reforming **58** 70
34. Wang C-y, Groenzin H and Shultz M J 2004 Direct observation of competitive adsorption between methanol and water on TiO_2: An in situ Sum-Frequency Generation Study *J. Am. Chem. Soc.* **126** 8094
35. Shen M and Henderson M A 2012 Role of water in methanol photochemistry on rutile TiO_2(110) *J. Phys. Chem. C* **116** 18788
36. Ohno T, Sarukawa K, Tokieda K and Matsumura M 2001 Morphology of a TiO_2 photocatalyst (Degussa, P-25) consisting of anatase and rutile crystalline phases *J. Catal.* **203** 82
37. Zhang J, Xu Q, Feng Z, Li M and Li C 2008 Importance of the relationship between surface phases and photocatalytic rutile TiO_2–Pd photocatalysts for hydrogen gas production from methanol reforming of TiO_2 *Angew. Chem. Int. Ed.* **47** 1766
38. Rothenberger G, Moser J, Graetzel M, Serpone N and Sharma D K 1985 Charge carrier trapping and recombination dynamics in small semiconductor particles *J. Am. Chem. Soc.* **107** 8054
39. Qian R, Zong H, Schneider J, Zhou G, Zhao T, Li Y, Yang J, Bahnemann D W and Pan J H 2018 Charge carrier trapping, recombination and transfer during TiO_2 photocatalysis: An overview *Catal. Today*
40. Choi W, Termin A and Hoffmann M (1994) The role of metal ion dopants in quantum-sized TiO_2: Correlation between photoreactivity and charge carrier recombination dynamics *J. Phys. Chem.* **98** 13669
41. Linsebigler A L, Lu G and Yates J T 1995 Photocatalysis on TiO_2 surfaces: Principles, mechanisms, and selected results *Chem. Rev.* **95** 735
42. Aas N, Pringle T J and Bowker M 1994 Adsorption and decomposition of methanol on TiO_2, $SrTiO_3$ and SrO *J. Chem. Soc. Faraday Trans.* **90** 1015
43. Addamo M, Augugliaro V, Di Paola A, García-López E, Loddo V, Marcì G and Palmisano L 2008 Photocatalytic thin films of TiO_2 formed by a sol-gel process using titanium tetraisopropoxide as the precursor *Thin Solid Films* **516** 3802
44. Oosawa Y and Grätzel M 1988 Effect of surface hydroxyl density on photocatalytic oxygen generation in aqueous TiO_2 suspensions *J. Chem. Soc. Faraday Trans. 1 Phys. Chem. Condensed Phases* **84** 197